Chains of coupled square dielectric optical microcavities

Manfred Hammer[*],
MESA$^+$ *Institute for Nanotechnology, University of Twente, Enschede, The Netherlands,*

Abstract: Chains of coupled square dielectric cavities are investigated in a 2-D setting, by means of a quasi-analytical eigenmode expansion method. Resonant transfer of optical power can be achieved along quite arbitrary, moderately long rectangular paths (up to 9 coupled cavities are considered), even with individual standing-wave resonators of limited quality. We introduce an ab-initio coupled mode model, based on a simple superposition of slab mode profiles as a template for the field of individual cavities. Although no loss mechanisms are built in, the model can still help to interprete the results of the former numerical experiments.
Keywords: integrated optics, numerical modeling, coupled mode theory, variational modeling, dielectric optical microcavities, resonator chains.
PACS codes: 42.82.–m 42.82.Bq 42.82.Et

1 Introduction

Coupled-resonator optical waveguides (CROWs) have been discussed already for some years as a means to realize waveguiding along paths with small-size bends, or for interest in their time-delay properties. A variety of concepts exist; among these are series of microring or -disk resonators [1, 2, 3], sequences of defects in photonic crystals or photonic crystal slabs [4, 5, 6], and coupled dielectric spheres [7, 8]. Some configurations can also be viewed as specific extended cases of photonic molecules [9, 10, 11].

As an alternative to the previous geometries, in this paper we take a look at chains of tiny dielectric cavities of *square* shape, that each support a single specific standing wave resonance [12, 13, 14] in the wavelength region of interest. Emphasis will be on the paths of the cavity sequences, with the aim of resonant transfer of optical power. Figure 1 introduces the configuration. In line with the fourfold symmetry of their resonant field pattern, the individual cavities are arranged sequentially on a discrete rectangular mesh, with conventional bus waveguides for guided-wave excitation and out-coupling at one end, or at both ends, of the chains.

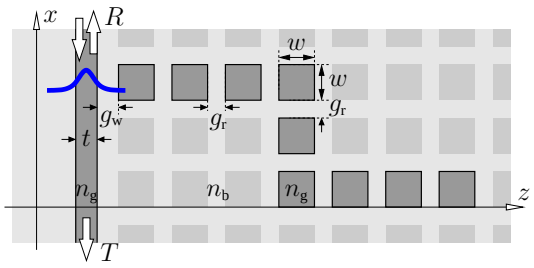

Figure 1: Resonator chain: a series of square high-index cavities of side length w, positioned on a rectangular equidistant grid (gray patches, homogeneous background) with spacing g_r. A bus waveguide of width t at a distance g_w is evanescently coupled to one end of the chain. n_g and n_b are the refractive indices of the cavity interior and waveguide core, and of the low index background. R and T indicate the relative reflected and transmitted modal power. The 2-D configurations are described in Cartesian coordinates x, z.

A rigorous semianalytical Helmholtz solver on the basis of local expansions into slab modes along two perpendicular axes (quadridirectional eigenmode propagation, QUEP [15, 16]) enables convenient numerical experiments on the rectangular, piecewise constant configurations. After the introductory example of Section 2, we consider variations of the length and shape of the chains in Section 3. The properties of a chain that connects two parallel bus waveguides are the subject of Section 4.

As some step towards an interpretation of the spectral features observed in the former examples, Section 5 introduces an intuitive coupled mode theory (CMT) model for the resonator chains. The overall field is assumed to consist of bidirectional versions of the guided mode of the bus core, with variable local amplitudes, together with the identical, properly positioned resonant field patterns of the individual cavities, each multiplied by a single scalar coefficient. These latter fields can be approximated quite well by a superposition of suitable slab mode profiles, oriented along the two coordinate axes [14]. Then one proceeds along the hybrid CMT approach

[*] *Department of Applied Mathematics, University of Twente P.O. Box 217, 7500 AE Enschede, The Netherlands*
Phone: +31/53/489-3448 Fax: +31/53/489-4833 E-mail: m.hammer@math.utwente.nl

(HCMT) of Ref. [17]: By variational means [18, 19, 20] one extracts a linear system of equations for the coefficients of the resonator fields, and for the amplitude functions of the bus modes, discretized in terms of finite elements, as unknowns. Section 5 compares the model with rigorous numerical calculations.

2 An initial example

We choose a rather arbitrary, but nontrivial double-bend arrangement of a chain with nine coupled individual cavities as an introductory example. The set of parameters, adapted from Ref. [14] and given in the caption of Figure 2, has been identified as appropriate for a setting with only one square cavity. At the design wavelength, one cavity with these properties exhibits a resonance of specific type (cf. Figure 3(1), Section 5.1, and Ref. [14]), while no further resonances[1] are supported in the wavelength range of interest (the spectral window in the figures below) by the single cavity.

All following numerical experiments rely on quasi-analytical simulations by means of the QUEP algorithm as described in Ref. [15]. The computational setting comprises a rectangular computational window with fully transparent boundaries (exception: the corner regions). These are placed, for each of the structures, by $3\,\mu$m away from the outermost dielectric interfaces, i.e. outside the regions that are shown in the field plots. Per slice and layer, the optical electromagnetic field is expanded into about 10 modes per μm width of the computational window, uniformly for all configurations in this paper. (Occasional) checks with respect to these simulation parameters indicate convergence of the results on the scale of the figures as given. Only 2-D configurations and TE polarized light are considered, the single nonvanishing electric component of the optical field is oriented perpendicular to the x-z-plane (cf. Figure 1). Figure 2 summarizes results for the S-bend chain.

We look at a spectral range around the design wavelength of $1.55\,\mu$m. The chain splits the single resonance of one individual cavity into a series of more or less well distinguished resonances, which show up as dips in the relative transmitted guided power T and simultaneous peaks in the relative reflected guided power R. These two quantities do not add up to one, hence a substantial amount of optical power is lost to nonguided waves (lossless dielectric materials are considered), that leave the computational window through the transparent boundaries.

One observes that for a major part the optical fields in each of the chains cavities are very similar to the shape of the resonance supported by a single dielectric square. We therefore evaluated "local amplitudes" for each cavity, the quantities A_0 – A_8, as a function of the wavelength, where the index indicates the position of the cavity in the chain, counting from the bus end. A_0 thus represents the intensity in the cavity that is connected to the bus waveguide. More specifically, A_j is the average of the squared local optical field at the eight spots close to the borders of the cavity core where the resonant field of the isolated single cavity would be at maximum. Even for the present configurations with rather pronounced losses, the relatively large intensities A_8 in the last cavity for the pattern c, d, and e indicate that an efficient resonant power transfer along the entire path of the chain is indeed feasible.

The field and intensity plots of Figure 2 illustrate the shape of the resonances. The field profiles represent time-snapshots of the principal y-component of the real, physical time harmonic electric fields, evaluated at a time within one period, when the maximum of the partly standing waves becomes visible (Alternatively: The overall phase of the complex fields has been chosen such that the spatial maximum of the real part is exhibited. Note that even with that adjustment the overall sign of profiles is still arbitrary). The intensity plots show the absolute square of the complex electric field. Gray levels are scaled to exhibit the local extrema of the individual pattern i.e. the scales are not comparable between different plots (cf. the curves of A_0 – A_8). These remarks apply also to all further images in this paper.

Necessarily, the static plots of Figure 2 can give only a rough impression of the rather complex behaviour of the optical electromagnetic field. It must be emphasized that, unlike the traveling waves observed in circular resonators, these are (almost) purely standing wave resonances: The time-domain view of the stationary, harmonically varying fields of the present chains shows as the major feature an in-place "$\pm$-blinking" of the field

[1] Due to mechanisms as outlined e.g. in Ref. [21, 14], the present standing-wave resonances do not occur as regularly as e.g. the almost periodic spectral features found for the traveling-wave whispering gallery modes of not too small dielectric rings or disks. Ref. [13] includes a plot of the spectral power transfer for a two-bus configuration with the parameters of Figure 7 over the larger window $\lambda \in [1.3, 1.7]\,\mu$m: the resonance in question is the only significant feature. Definition of a free spectral range seems not appropriate in that case.

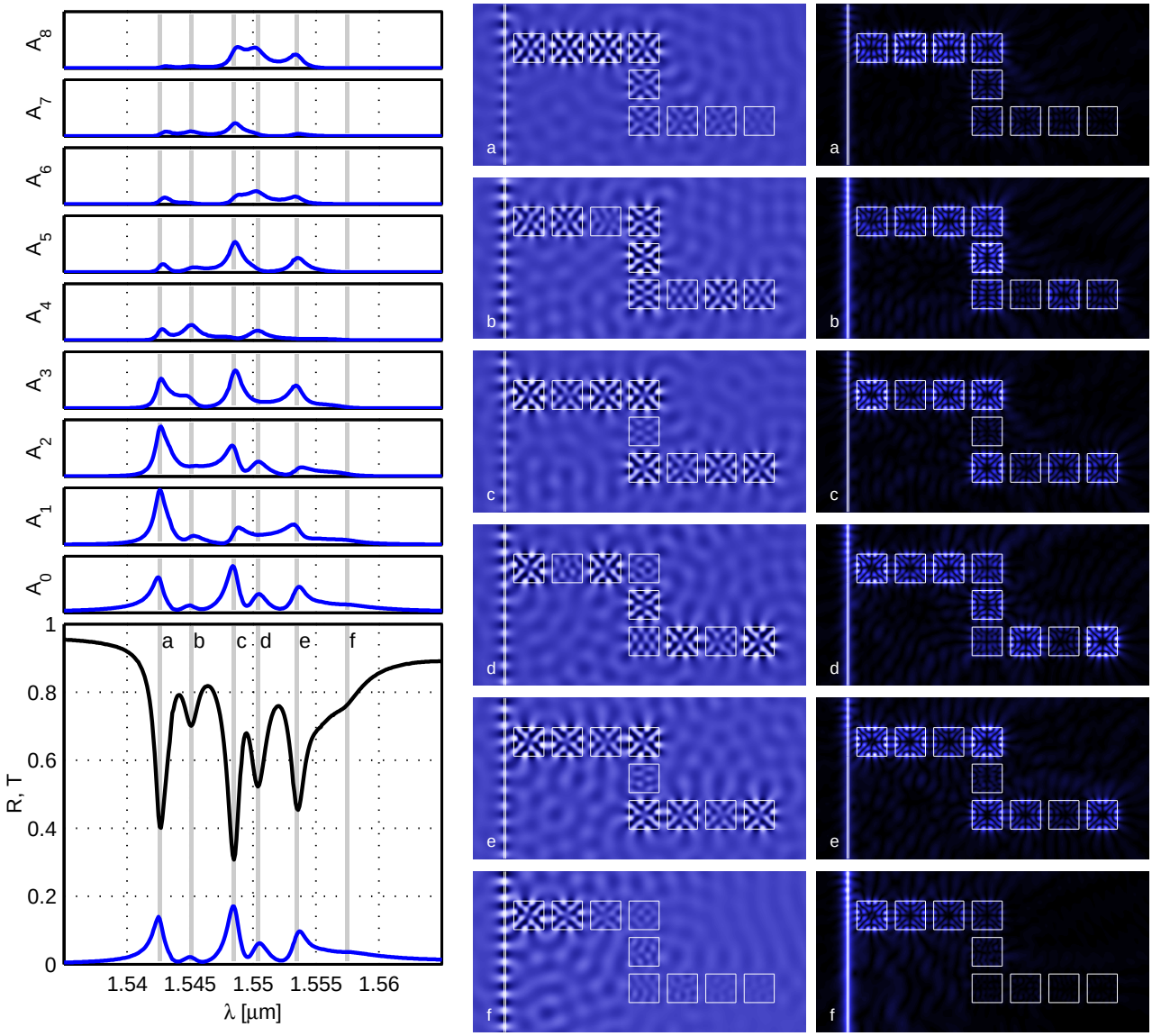

Figure 2: A double-bend chain with nine square cavities. Parameters, as introduced in Figure 1: $n_b = 1.45$, $n_g = 3.40$, $t = 0.073\,\mu$m, $w = 1.451\,\mu$m, $g_w = g_r = 0.4\,\mu$m. *Left column: reflected power* R *and transmitted power* T *in the bus waveguide (bottom), and local field intensities* $A_0 - A_8$ *in the individual cavities, counting from the input end. Center and right column: field snapshots (center) and optical intensity profiles (right) for the wavelengths (letters a – f) indicated by the gray vertical lines in the spectral plots.*

in each cavity, where the horizontal, vertical, and diagonal nodal lines stay in place. Extremal field strengths in different cavities appear at different moments within the time period. Traveling waves, or partly traveling waves, are observed in the bus waveguide, and outside the cavity and bus cores. The latter contribute to the radiation losses of the structure, if they cross the windows of the computational boundaries, but they could also be a cause of a "large distance", non-next-neighbor interaction between the cavities.

3 Chain properties

With length and shape we restrict to the two most obvious "parameters" that specify the chain path. Certainly also the influence of other quantities can be of interest. These would be the variables that influence the resonances of individual cavities (refractive index contrast, width / aspect ratio; other shapes or distortions), quantities that determine the interaction between the cavities (distance, positioning, not necessarily on a rectangular grid), and the parameters that specify the excitation conditions (gap, bus waveguide parameters). If limited to rectangular 2-D configurations, the corresponding studies could be carried out with the methods as used in this paper. One would not necessarily have to restrict to uniform changes of the variables as introduced in Figure 1: There are indications [7, 22] that more irregular changes of e.g. sizes or distances of individual

cavities could be promising just as well. However, given the properties of an individual (optimized) square and its resonance wavelength, we experienced that, beyond choosing plausible values for the gaps between the cavities, for the gap between bus core and the input cavity, and for the width of the bus waveguide[2] no particular further design strategy was necessary to realize the chain resonances discussed in this section.

3.1 Length of the chain

Figure 3 summarizes the spectral properties of straight chains of lengths up to nine, and examples for resonant field profiles for short chains. With growing length, the pattern found for the larger structures appear to evolve from the single feature in the spectrum of the one-cavity "chain", and the related extremal field. There are no specific differences between chains with even or odd numbers of squares[3].

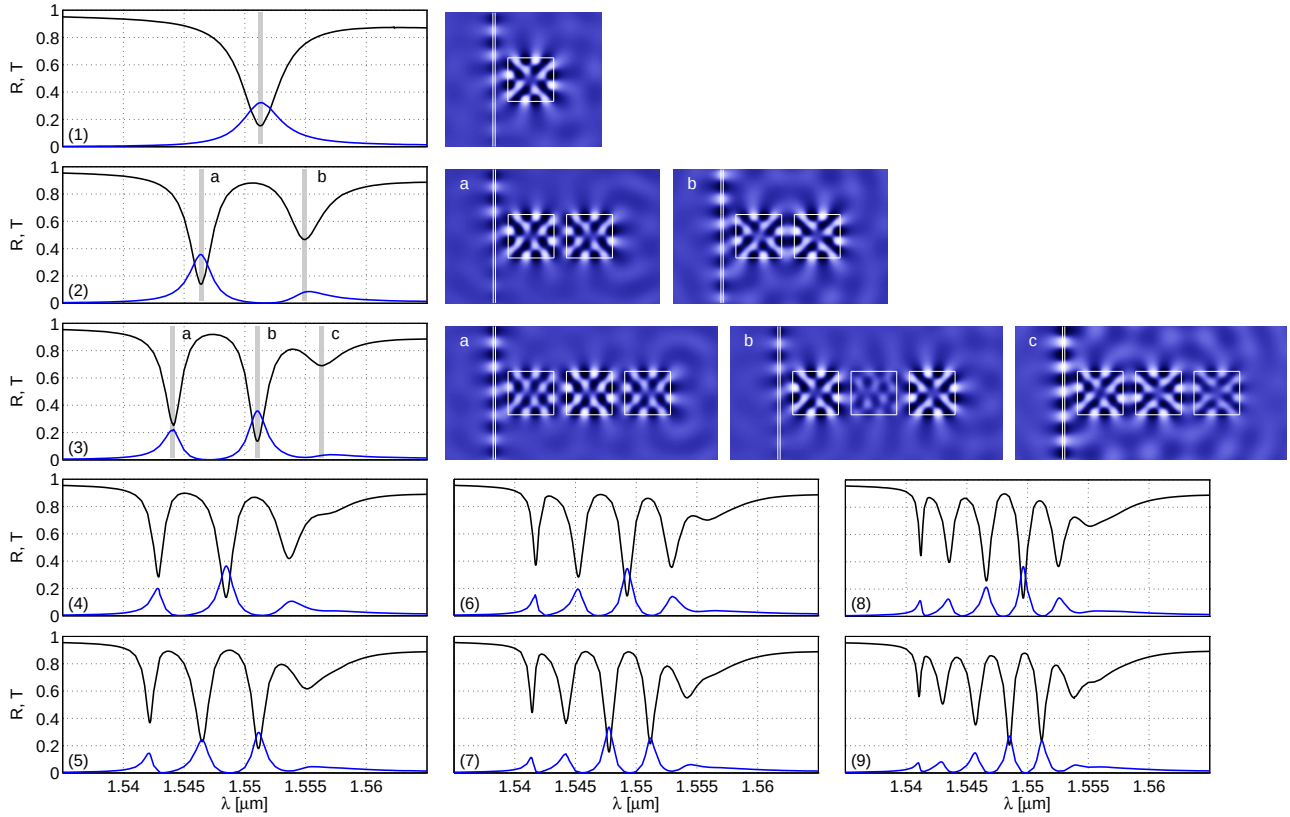

Figure 3: Straight chains of lengths one (1) up to nine (9) with the parameters of Figure 2. The plots show the guided wave reflection R and transmission T versus the excitation wavelength λ, and, for chains of length (1), (2), and (3), snapshots of the resonant field pattern at the wavelengths indicated by the gray vertical lines in the spectra.

One observes an increase in the number of spectral peaks with the number of cavities. The interaction between the squares in the composite structures splits the single resonance of the one-cavity chain into several features close to the original wavelength. Examination of the resonant fields reveals a common "supermode" phenomenon (cf. e.g. Ref. [24] for a discussion of CROW supermodes), where the extremal profiles supported by the composite, longer chains are made up from properly placed copies of the single-cavity field, superimposed systematically with specific relative amplitudes. Denoting the single cavity mode, with a phase / sign as shown, by a symbol $[+]$, the supermodes of the two-cavity chain could be classified as $[++]$ (a) and $[+-]$ (b), respectively. Correspondingly, one would write the symbols $[+\,+\,+]$ (a), $[+0-]$ (b), and $[+\,-\,+]$ (c) for the resonances of the three-cavity chain. Note that here the fundamental excitations, the ones that show up at the largest wavelength or the lowest frequency ("energy") are the ones with the *least* symmetric vectors of amplitudes, i.e. resonances (b) for the two-cavity and (c) for the three cavity chain: Due to the antisymmetry of the single-cavity profile, these composite fields show less "nodes", vertical nodal lines in the gaps between

[2] Here a phase matching argument involving the access mode and one of the modes that contribute to the cavity resonance (cf. Section 5) can be helpful [14].

[3] In case of a filter setting with two parallel chains between two bus waveguides, symmetry properties (i.e. also the chain length) might well be significant [23].

cavities, than the other supermodes.

While this discussion should apply more or less analogously also for the longer chains, losses come into play, such that the individual spectral peaks start to overlap, such that already for the four cavity chain one can hardly identify all four expected resonances.

3.2 Chain shape

Due to the specific symmetry and strong confinement of the field in the individual cavities one might expect that the particular shape of the chain does not matter as long as it can still be viewed as one sequence with one loose end. Figure 4 compares spectra and resonance pattern of chain configurations with length nine along different paths with one, two, or three bends. The field plots show the resonances at the wavelength of the peak in the transmission pattern that is closest to the most pronounced resonance (c) of Figure 2. Note that also the straight chain (9) of Figure 3 could be grouped into this series.

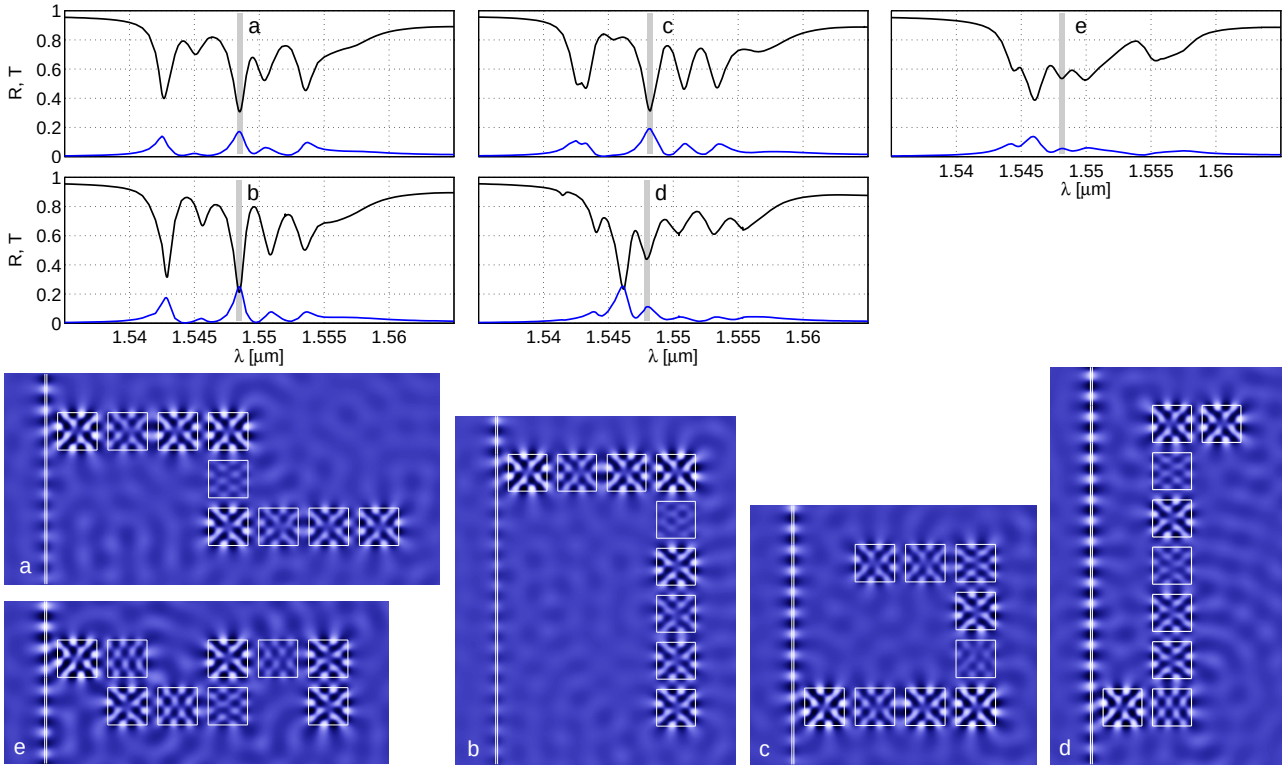

Figure 4: Spectral guided wave reflection R and transmission T for chains of length nine with different sequential placement of the squares. Parameters are as introduced in Figure 2. The plots (a) to (d) of specific resonant fields indicate the respective shape of the chains.

Obviously the shape of the chain path *has* some influence on the spectral response of the present configurations. Effects like corner coupling and radiative or evanescent “long distance” interaction are apparently relevant, not only the next neighbor interaction.

4 Two bus waveguides

The observation of quite high field levels at the loose end of the former structures raises immediately the question, whether the chain can be linked to two bus waveguides, as a means to realize a resonant transfer of optical power between them. Figure 5 shows the spectral power transmission of a straight configuration with nine cavities, Figure 6 illustrates the fields that establish at some of the resonances.

The spectral curves of Figure 5 adhere to the scheme stated for standing wave resonators in [12]: Off resonance, the input power merely travels down the input bus waveguide, here to output port B. At resonance, a certain part of this input excites the field in the cavity, which in turn distributes this power equally among the four

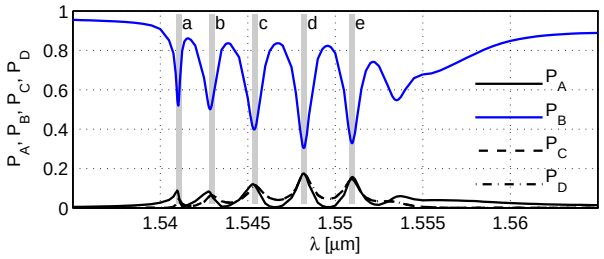

Figure 5: Spectral power transmission of a straight nine-cavity chain between two parallel bus waveguides, with parameters as given for Figures 1 (symmetric, straight arrangement) and 2. The quantities P_A – P_D are the guided relative output powers received by ports A – D upon excitation in port A, as introduced in the plots of Figure 6.

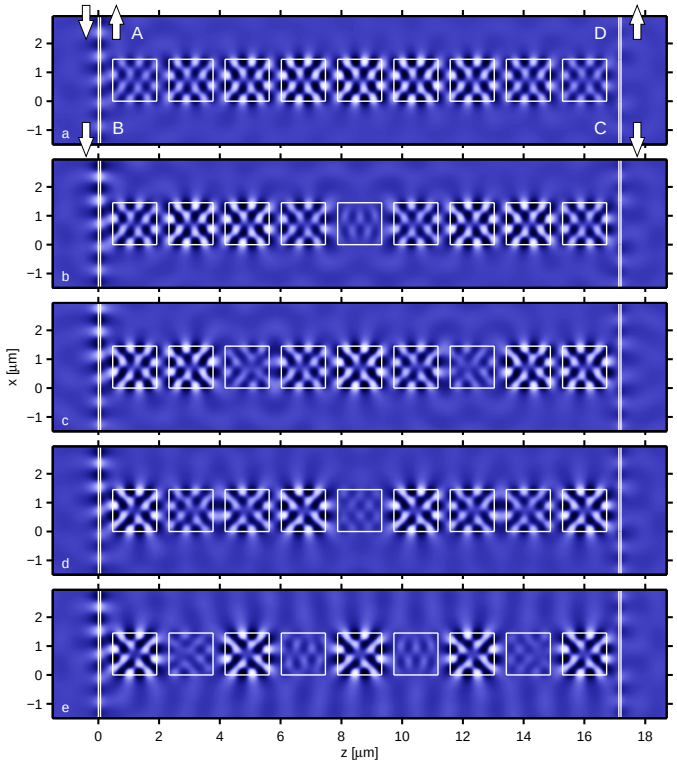

Figure 6: Shapes of resonant fields supported by the straight nine-cavity chain coupled to two bus waveguides. Plots (a) – (e) correspond to the wavelengths indicated by the gray vertical lines in Figure 5.

output ports, where in ports A and B superpositions with the incoming / the directly transmitted waves are present. Although the extremum of 25% transmission to all ports is not reached, the present configurations are not too far off this limit. A structure with only a single "connection" between the bus waveguides is hence only partly useful as a wavelength filter device, since at most a quarter of the input arrives at the drop ports C or D. Two coupled parallel connections [12, 13] could offer a way out; corresponding (abstract) concepts have been discussed in [25, 23].

With the introduction of the second bus waveguide the structure is now fully symmetric with respect to the center of the middle cavity. This symmetry shows up nicely in the properties of the series of supermodes as shown in Figure 6, where the systematic mentioned in Section 3.1 applies as well.

5 HCMT model

Although somewhat obscured at some instances by quite pronounced losses, the phenomena observed in the former series of examples are more or less as expected for a sequential arrangement of coupled oscillators. Still, while "modes of individual cavities" and their "interaction" play a role in the previous discussion, merely the numbers from the QUEP simulations can hardly justify the use of these notions. Therefore, this section tries to found the interpretation on an approximate coupled mode model, which allows to quantify that viewpoint: The applicability range of the model below is defined by how close the ansatz (2) comes to physical reality. A complete failure of the model would imply that the former interpretation is entirely inappropriate. Shortcomings in certain aspects indicate that these aspects are not well represented in the template (2) or in its ingredients. Note that, although the almost analytical HCMT model requires a by far lower computational effort than the QUEP reference calculations, it is here meant to complement, not to replace the latter (cf. the remarks at the

end of Section 5.3 for comments on possible improvements).

To allow for some better chance of an also quantitative comparison we choose a set of parameters similar to Refs. [12, 13] with even higher refractive index contrast, such that losses can be expected to have a less significant influence. We shall see that the observations from the HCMT/QUEP comparison lead to an interpretation that applies also to the spectral features found in Section 2. Application of the formalism below directly to the structure of Section 2 yields results that resemble qualitatively the HCMT data in Figure 9; the relation to the reference of Figure 2 would be even less obvious, however.

5.1 Field template

The description in terms of coupled mode theory (CMT) starts with identifying a suitable, if necessary approximate, expression for the resonant optical field supported by an individual square cavity. Figure 7 shows that field for the new parameter set. Note that only that single resonance appears within the wavelength range of interest.

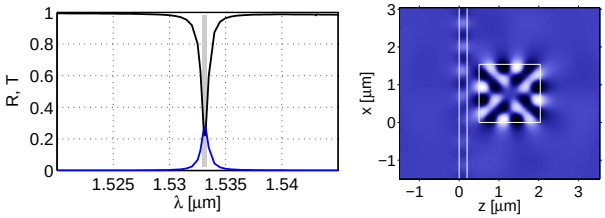

Figure 7: Spectral power transfer (left) and field profile at resonance $\lambda = 1.5331\,\mu m$ (right) of a single dielectric square coupled to one bus waveguide. Parameters (cf. Figure 1): $n_b = 1.0$, $n_g = 3.2$, $w = 1.54\,\mu m$, $g_r = 0.39\,\mu m$, $g_w = 0.3\,\mu m$, $t = 0.2\,\mu m$; design wavelength $\lambda_0 = 1.532\,\mu m$.

The reasoning of Refs. [21, 14] suggests that a superposition of suitable slab mode profiles could be useful at this point. One considers the symmetric multimode slab that corresponds to either the vertical or horizontal refractive index cross section of our square, and computes, at the design wavelength close to the former resonance, its guided modes of third order η_0 and fifth order η_1. Then indeed, according to Figure 8, the antisymmetric 2-D superposition

$$\psi(x,z) = \eta_0(x)\,\eta_1(z) - \eta_1(x)\,\eta_0(z) \tag{1}$$

of these functions results in a profile ψ that appears to be very similar to the shape of the resonance in Figure 7. ψ can thus serve as the prototype for the mode of a single cavity.

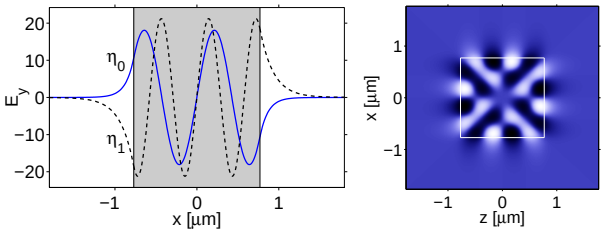

Figure 8: Left: Third and fifth order guided TE mode profiles of a symmetric three-layer dielectric slab with refractive indices n_b, n_g, and thickness w at wavelength λ_0, principal electric component E_y. Right: A specific totally antisymmetric 2-D superposition ψ of the two former profiles η_0 and η_1 (cf. the text).

We now consider again the S-bend chain configuration with nine cavities. For what follows it is helpful to extend ψ to an approximation $\boldsymbol{\psi}$ for the full optical electromagnetic field of a single cavity, by applying the superposition formula also to the magnetic slab mode components. Further, one copy $\boldsymbol{\psi}_j$ of this field is introduced for each cavity $j = 0, \ldots, 8$, shifted to the respective cavity center position. Then we assume that the optical electromagnetic field in the chain is well represented by the template

$$\begin{pmatrix} \boldsymbol{E} \\ \boldsymbol{H} \end{pmatrix}(x,z) = u(x)\,\boldsymbol{\phi}_{\mathrm{u}}(x,z) + d(x)\,\boldsymbol{\phi}_{\mathrm{d}}(x,z) + \sum_{j=0}^{8} r_j\,\boldsymbol{\psi}_j(x,z). \tag{2}$$

Here $\boldsymbol{\phi}_{\mathrm{u}}$ and $\boldsymbol{\phi}_{\mathrm{d}}$ are the — known — upwards and downwards traveling variants of the guided bus modes, the z-dependent mode profiles multiplied by the respective exponential dependence on their propagation coordinate x. Due to the interaction with the chain the contribution of these modes to the overall field will change along the vertical coordinate, therefore x-dependent amplitude functions u and d are introduced. Together with the coefficients r_j of the fields $\boldsymbol{\psi}_j$ associated with the individual squares, these are the unknowns in Eq. (2).

5.2 Solution procedure

In order to apply the procedures of the hybrid analytical/numerical CMT variant (HCMT) of Ref. [17], the unknown functions u and d are discretized by 1-D linear finite elements. Discrete coefficients u_l, d_l replace the functions, such that the template (2) assumes the abstract form

$$\begin{pmatrix} \boldsymbol{E} \\ \boldsymbol{H} \end{pmatrix}(x,z) = \sum_k a_k \, \boldsymbol{\chi}_k(x,z). \tag{3}$$

Here $\boldsymbol{\chi}_k$ are either directly the functions $\boldsymbol{\psi}_j$, or modal elements, i.e. products of the mode field (profile times exponential propagation term) and the hat function of the respective element. $a_k \in \{u_l, d_l, r_j\}$ are the corresponding unknown coefficients, with an abstract index k that covers the bus mode propagation directions, the element numbers, and the indices of the individual cavities.

Basis for the following procedure is then the variational representation of the Helmholtz problem on a suitable 2-D domain that covers the interesting region around the structure, with transparent-influx-boundary conditions that account for the outgoing half-infinite pieces of the bus waveguides in the exterior [17]. By restricting the corresponding functional to the discretized field template (3) and looking for vectors of coefficients a_k at which the restricted functional becomes stationary, a small to moderate sized system of linear equations for the a_k can be obtained (only 1-D FEM discretizations are involved). The numerical solution gives a set of coefficients that allows to assemble an approximation to the full optical field. Besides the guided power transmission, the local amplitudes of the directional modes in the bus waveguide, and the coefficients assigned to the fields of the individual cavities can be directly inspected. Full details of the approach are given in Ref. [17].

So far the frequency ω has been treated as a fixed parameter. Spectral properties are computed as scans over ω, while keeping the functions η_0, η_1 and hence also $\boldsymbol{\psi}_j$ fixed at the mode profiles that were determined for the design wavelength. This implements the notion that the properties of the chain are determined as interactions of specific resonant modes supported by the individual cavities, each with a fixed associated resonance frequency.

5.3 HCMT results

According to Figure 9, the present parameter set leads to less pronounced dips in the transmission, but at the same time to sharper, better separated resonances, when compared with Figure 2. Still the quantitative agreement of the rigorous QUEP simulations with the approximate model is only quite moderate. At least the HCMT predicts a series or resonances in the appropriate region, and the resonant field profiles, as far as identifiable, share common major features such as e.g. the occurrence of small field strengths at certain positions in the chain.

The features in the HCMT spectrum are sharp and pronounced, with a spectral width that is purely determined by the interaction with the bus waveguide. The field patterns corresponding to these well separated resonances could thus be viewed as approximations to the supermodes supported by the entire chain, the coupled resonant modes of the individual cavities, superimposed with specific wavelength dependent relative amplitudes. The HCMT results show a systematics in the supermode forms, i.e. in the distribution of relative amplitudes r_j over cavity positions j throughout the series (a) - (i) of resonances, as observed in Section 3.1.

The time domain view on the stationary, time-harmonic fields reveals that the rather irregular “blinking” pattern mentioned in Section 2 is for the present case replaced by a simultaneous change of field amplitudes in all cavities, where extremal levels appear at more or less the same moment in all cavities, in line with the almost real supermode amplitudes as predicted by the HCMT model.

A (slightly speculative) comparison of the HCMT and QUEP results of the present high-contrast configuration with the initial observations of Figure 2 could lead to the following interpretation of the former, more irregular data: A sequence of nine supermodes are also supported by the former structure with lower contrast; they suffer, however, from much stronger losses, such that their contributions to the spectral transmission partly overlap. The feature (a) in Figure 2 would thus include contributions from two supermodes of shapes according to resonances (a) and (b) in Figure 9. Note that an interference of the sequences (a) and (b) of coefficients r_j in Figure 9 with suitable relative amplitudes can be constructive in the first half of the chain, and destructive in the second half. Then, with some good will, the sequence (b), (c), (d), and (e) of shapes in Figure 2 corresponds to

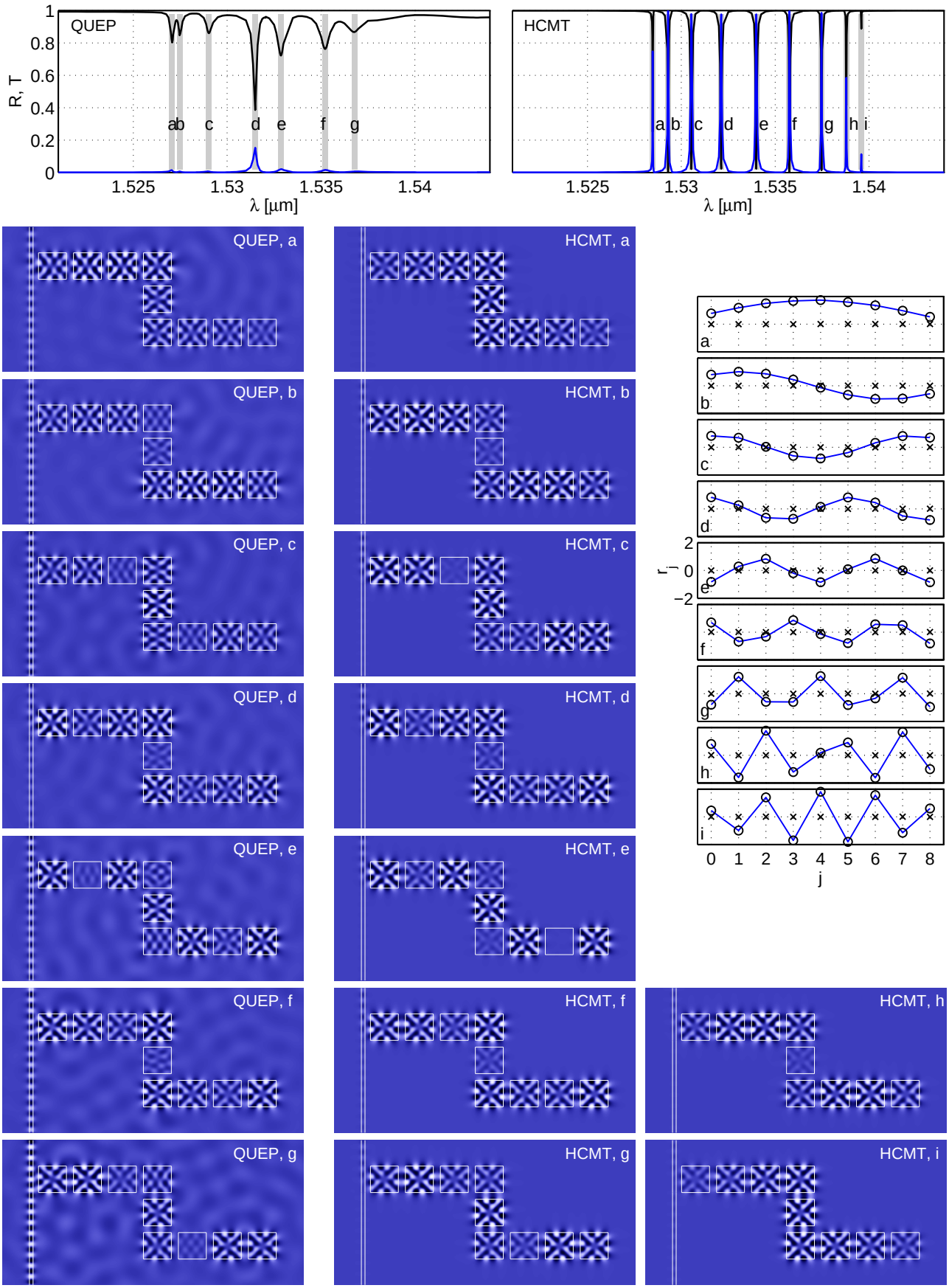

Figure 9: For an S-bend nine-cavity chain with parameters as given for Figure 7: Spectral guided wave reflection and transmission, and resonant field pattern, as predicted by the rigorous numerical simulations (QUEP, left) and by the approximate CMT model (HCMT, right). The middle right inset shows the complex coefficients r_j (circles / crosses: real and imaginary parts) with which the the individual cavities (index j; $j = 0$: the bus end of the chain) contribute to the supermodes (a) – (i).

the profiles (c), (d), (e), and (f) of Figure 9. Lossy resonances with shapes similar to (g), (h), and (i) of Figure 9 might contribute to the shoulder (f) of Figure 2.

The adequate incorporation of optical radiation losses is probably crucial for a quantitative improvement of the CMT model. This would require to provide fields for the actual lossy eigenmodes (leaky modes, quasi-normal modes) of the individual cavities. These would be the complex frequency eigensolutions of the open, homogeneous Helmholtz problem. An example for coupled quasi-normal modes supported by defects in 1-D multilayer stacks is given in Refs. [26, 27]. 2- or 3-D configurations require numerical approximations, where solvers for the field shapes and complex eigenfrequencies of open dielectric cavities are less frequently found. Among the few examples are the FEM modules in the commercial package [28], and academic programs of more numerical [19] (FEM) or analytical character [29, 30, 10] (circular cavities). Probably also the near field solutions at resonances (scattered field part) generated by a computational treatment of specific scattering problems [31, 32, 24], for individual, suitably shaped cavities could be used for this purpose. A third alternative would be to employ real-frequency eigensolutions for the open, leaky individual cavities with artificial gain ("lasing eigenvalue problem" [33, 34]).

6 Concluding remarks

Sequential arrangements of square 2-D dielectric optical microcavities have been considered, with one or two ends of the chains coupled evanescently to straight dielectric waveguides that function as input/output ports. Rigorous numerical simulations show that a resonant transfer of optical power along chains of quite arbitrary shape, including rectangular bends, is feasible, even with individual cavities of moderate quality. By varying the shape of the chain path, it was found that a next-neighbor interaction is not sufficient to explain the changes in the power transfer spectrum. Apparently an evanescent or radiative long distance interaction plays a role for the present, not too unrealistic set of design parameters. When looking at chains of growing length we could observe a systematic characteristic of supermode excitation, i.e. collective oscillations of all cavities, and the corresponding splitting of the resonance frequency associated with a single dielectric square.

Our hybrid coupled mode model permits to explain at least some major features of these — at a first glance rather irregular — spectral properties. No free parameters are introduced. The model, however, disregards any radiative losses (so far), and thus cannot be more than an approximation of the resonator chain in a kind of high-Q limit. Note that an extension of the chain, with just one additional unknown per cavity, does hardly imply any additional computational burden for the HCMT model. With a more realistic template for the leaky cavity modes, this could open a way for an adequate treatment of really long chains.

This is admittedly a somewhat academic example, in so far as only the simplest case of 2-D configurations are considered. Still, just as for most concepts discussed nowadays for photonic crystal slabs, it remains to be seen whether these results are relevant for realistic, necessarily high-contrast slab-like 3-D devices.

So far we didn't pay any attention to time-domain properties of the light propagation along the chains. Corresponding studies could concern the slow transfer of light pulses along the chain path [35, 36], or the time delay properties [3, 37] of a chain when attached to one branch in an interferometer setting.

Acknowledgments

This work has been supported by the Dutch Technology foundation (BSIK / NanoNed project TOE.7143). The author thanks E. van Groesen, H. J. W. M. Hoekstra, O. V. Ivanova, M. Maksimovic, and R. Stoffer for many fruitful discussions.

References

[1] A. Yariv, Y. Xu, R. K. Lee, and A. Scherer. Coupled-resonator optical waveguide: a proposal and analysis. *Optics Letters*, 24(11):711–713, 1999.

[2] B. E. Little, S. T. Chu, P. P. Absil, J. V. Hryniewicz, F. G. Johnson, F. Seiferth, D. Gill, V. Van, O. King, and M. Trakalo. Very high-order microring resonator filters for WDM applications. *IEEE Photonics Technology Letters*, 16(10):2263–2265, 2004.

[3] F. Morichetti, A. Melloni, A. Breda, A. Canciamilla, C. Ferrari, and M. Martinelli. A reconfigurable architecture for continuously variable optical slow-wave delay lines. *Optics Express*, 15(25):17273–17281, 2007.

[4] M. Bayindir, B. Temelkuran, and E. Ozbay. Propagation of photons by hopping: A waveguiding mechanism through localized coupled cavities in three-dimensional photonic crystals. *Physical Review B*, 61(18):R11 855–R11 858, 2000.

[5] A. L. Reynolds, U. Peschel, F. Lederer, P. J. Roberts, T. F. Krauss, and P. J. I. de Maagt. Coupled defects in photonic crystals. *IEEE Transactions on Microwave Theory and Techniques*, 49(10):1860–1867, 2001.

[6] J. Scheuer, G. T. Paloczi, J. K. S. Poon, and A. Yariv. Coupled resonator optical waveguides — toward the slowing & storage of light. *Optics & and Photonics News*, 16(2):36–40, 2005.

[7] V. N. Astratov, J. P. Franchak, and S. P. Ashili. Optical coupling and transport phenomena in chains of spherical dielectric microresonators with size disorder. *Applied Physics Letters*, 85(23):5508–5510, 2004.

[8] Z. Chen, A. Taflove, and V. Backman. Highly efficient coupling and transport phenomena in chains of dielectric microspheres. *Optics Letters*, 31(03):389–391, 2006.

[9] S. V. Boriskina. Efficient simulation and design of coupled optical resonator clusters and waveguides. Proceedings of the 7th International Conference on Transparent Optical Networks (ICTON), Vol. 2, 330–332, 2005.

[10] S. V. Boriskina. Spectrally engineered photonic molecules as optical sensors with enhanced sensitivity: aproposal and numerical analysis. *Journal of the Optical Society of America*, 23(8):1565–1573, 2006.

[11] S. V. Boriskina, T. M. Benson, and P. Sewell. Photonic molecules made of matched and mismatched microcavities: new functionalities of microlasers and optoelectronic components. Proceedings of SPIE, Vol. 6452, 64520X, 2007.

[12] C. Manolatou, M. J. Khan, S. Fan, P. R. Villeneuve, H. A. Haus, and J. D. Joannopoulos. Coupling of modes analysis of resonant channel add-drop filters. *IEEE Journal of Quantum Electronics*, 35(9):1322–1331, 1999.

[13] M. Lohmeyer. Mode expansion modeling of rectangular integrated optical microresonators. *Optical and Quantum Electronics*, 34(5):541–557, 2002.

[14] M. Hammer. Resonant coupling of dielectric optical waveguides via rectangular microcavities: The coupled guided mode perspective. *Optics Communications*, 214(1–6):155–170, 2002.

[15] M. Hammer. Quadridirectional eigenmode expansion scheme for 2-D modeling of wave propagation in integrated optics. *Optics Communications*, 235(4–6):285–303, 2004.

[16] M. Hammer. METRIC — Mode expansion tools for 2D rectangular integrated optical circuits. http://www.math.utwente.nl/∼hammerm/Metric/.

[17] M. Hammer. Hybrid analytical / numerical coupled-mode modeling of guided wave devices. *Journal of Lightwave Technology*, 25(9):2287–2298, 2007.

[18] C. Vassallo. *Optical Waveguide Concepts*. Elsevier, Amsterdam, 1991.

[19] A. Sopaheluwakan. *Characterization and Simulation of Localized States in Optical Structures*. University of Twente, Enschede, The Netherlands, 2006. Ph.D. Thesis.

[20] E. W. C. van Groesen and J. Molenaar. *Continuum Modeling in the Physical Sciences*. SIAM publishers, Philadelphia, USA, 2007.

[21] M. Hammer and E. van Groesen. Total multimode reflection at facets of planar high contrast optical waveguides. *Journal of Lightwave Technology*, 20(8):1549–1555, 2002.

[22] S. V. Boriskina. Coupling of whispering-gallery modes in size-mismatched microdisk photonic molecules. *Optics Letters*, 32(11):1557–1559, 2007.

[23] S. Fan, P. R. Villeneuve, J. D. Joannopoulos, M. J. Khan, C. Manolatou, and H. A. Haus. Theoretical analysis of channel drop tunneling processes. *Physical Review B*, 59(24):15882–15892, 1999.

[24] S. V. Pishko, P. D. Sewell, T. M. Benson, and S. V. Boriskina. Efficient analysis and design of low-loss whispering-gallery-mode coupled resonator optical waveguide bends. *Journal of Lightwave Technology*, 25(9):2487–2494, 2007.

[25] M. J. Khan, C. Manolatou, S. Fan, P. R. Villeneuve, H. A. Haus, and J. D. Joannopoulos. Mode-coupling analysis of multipole symmetric resonant add/drop filters. *IEEE Journal of Quantum Electronics*, 35(10):1451–1460, 1999.

[26] M. Maksimovic, M. Hammer, and E. van Groesen. Field representation for optical defect microcavities in multilayer structures using quasi-normal modes. *Optics Communications*, 281(6):1401–1411, 2008.

[27] M. Maksimovic, M. Hammer, and E. van Groesen. Coupled optical defect microcavities in 1d photonic crystals and quasi-normal modes. In C. M. Greiner and C. A. Waechter, editors, *Integrated Optics: Devices, Materials, and Technologies XII*, volume 6896 of SPIE Proceedings, pages 689605–1 – 689605–11, 2008.

[28] JCMwave GmbH, Haarer Str. 14a, 85640 Putzbrunn/Munich, Germany; http://www.jcmwave.com/ .

[29] L. Prkna, J. Čtyroký, and M. Hubálek. Ring microresonator as a photonic structure with complex eigenfrequency. *Optical and Quantum Electronics*, 36(1/3):259–269, 2004.

[30] L. Prkna. *Rotationally symmetric resonant devices in integrated optics*. Faculty of Mathematics and Physics, Charles University, Prague, and Institute of Radio Engineering and Electronics, Academy of Sciences of the Czech Republic, Prague, Czech Republic, 2004. Ph.D. Thesis.

[31] S. V. Boriskina, P. Sewell, T. M. Benson, and A. I. Nosich. Accurate simulation of two-dimensional optical microcavities with uniquely solvable boundary integral equations and trigonometric galerkin discretization. *Journal of the Optical Society of America A*, 21(03):393–402, 2004.

[32] S. V. Boriskina, T. M. Benson, P. Sewell, and A. I. Nosich. Optical modes in 2-d imperfect square and triangular microcavities. *IEEE Journal of Quantum Electronics*, 41(6):857–862, 2005.

[33] E. I. Smotrova and A. I. Nosich. Mathematical study of the two-dimensional lasing problem for the whispering-gallery modes in a circular dielectric microcavity. *Optical and Quantum Electronics*, 36:213–221, 2004.

[34] E. I. Smotrova, A. I. Nosich, T. M. Benson, and P. Sewell. Optical coupling of whispering-gallery modes of two identical microdisks and its effect on photonic molecule lasing. *IEEE Journal of Selected Topics in Quantum Electronics*, 12(1):78–85, 2006.

[35] F. Melloni, A. andd Morichetti and M. Martinelli. Linear and nonlinear pulse propagation in coupled resonator slow-wave optical structures. *Optical and Quantum Electronics*, 35:365–379, 2003.

[36] J. K. S. Poon, L. Zhu, G. A. DeRose, and A. Yariv. Transmission and group delay of microring coupled-resonator optical waveguides. *Optics Letters*, 31(4):456–458, 2006.

[37] F. Morichetti, A. Melloni, C. Ferrari, and M. Martinelli. Error-free continuously-tunable delay at 10 Gbit/s in a reconfigurable on-chip delay line. *Optics Express*, 16(12):8395–8399, 2008.